COMPUTATIONAL ANALYSIS OF CD NOZZLE FOR SOLID PROPELLANT ROCKET

Mohammed iliyaas .A
PG Student Aeronautical Engineering ,
Anna University Tirunelveli Region, Tirunelveli,

Dr.K.Karuppasamy
Assisant Professor, Department Of Mechanical Engineering,
Anna University Tirunelveli Region, Tirunelveli.

Abstract- The converging-diverging nozzles play a significant role in a supersonic missile and rocket, where they using in retro rockets also too. Due to the back pressure conditions through the convergent section, air reaches sonic conditions at throat. These conditions lead this stream to flow further through the divergent section where the flow Mach number increases using pressure differences. Manipulating the determinative variables such as area ratio and back pressure, the obtained Mach number may be regulated. In the present work a comprehensive simulation of a flow in a typical supersonic converging-diverging nozzle has been analyzed. In the respective nozzle, flow suddenly contracts at a certain point and then expands after throat. All the simulation endeavors have been carried out by ANSYS FLUENT® utilizing the mesh geometries previously and precisely accomplished in ANSYS WORKBENCH®. The simulations have been conducted in 2D domains to provide better platform. Also, the influence of the turbulence model, differentiation and computational grid to the solution has been studied. Furthermore, the numerical comparison between CFD Modeling results and corresponding available measured data has been presented. The comparison analysis of the data demonstrates an accurate enough coordination between the experimental data and the computational simulation results, which is applied in 2Ds**.**

Keywords: *ANSYS FLUENT®, computational fluid dynamics, converging-diverging nozzle, turbulence models.*

I. INTRODUCTION

A nozzle is a proportionally plain device, specifically a formed tube which can lead hot and fast gases through. Aerospace shuttles basically use a fixed convergent section followed by a fixed divergent section as the configuration design of the nozzle [1]. There are different applications where nozzle is used to accelerate hot exhaust to generate thrust which works based on the Newton's 3rd law of motion such as in Ramjets, scramjets, and rockets [2]. Nozzle design specifies the amount of thrust since for different nozzle designs, several parameters such as mass flow rate, outlet pressure and outlet velocity of the engine might be various [3], [4] Based on the configurations, nozzles can be divided into three general types:

1) Cone nozzles which are conical and linear [5];
2) Bell nozzles which are contoured, shaped and classical converging-diverging [6];
3) Annular nozzles which are spike, aerospike, plug, expansion and expansion-deflection [7].

Each of the mentioned nozzles has advantages and disadvantages against the others and according to the configurations, each could be beneficial for different applications [8]. The nozzle configuration which is the topic of this research is converging-diverging nozzle. Converging-diverging nozzle was first used on steam turbines by a Swedish inventor called Gustaf de Laval which is now also well known as de Laval nozzle or Converging-Diverging Nozzle [9]. In a converging- diverging nozzle, the hot exhaust

leaves the combustion chamber and converges down to the minimum area, or throat, of the nozzle. The converging part is subsonic while in the throat Mach number is 1 and in the diverging part it reaches over unity. Mach number usually increases even after throat to the end while in some cases a small decrease in Mach number has been reported [10]. When the back pressure ratio is large enough, the flow within the entire device will be subsonic and isentropic. When the back pressure ratio reaches a critical value, the flow will become choked with subsonic flow in the converging section, sonic flow at the throat, and subsonic flow in the diverging section[11].

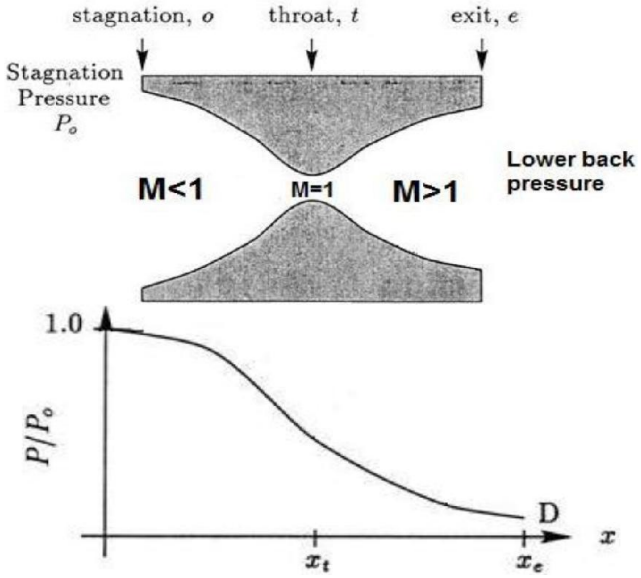

Fig. 1. Schematic view and a qualitative diagram of pressure versus the length axis for a converging-diverging nozzle with fully supersonic flow [1].

Basically, a supersonic converging-diverging nozzle has two sorts of flow trends:

1) Fully supersonic flow (M>1): As shown in Fig.1, nozzle is choked; flow accelerates through the converging section, reaches its maximum speed at the throat and accelerates through the diverging section [12].

2) Shock wave (supersonic flow with shock wave): As illustrated in Fig. 2, nozzle is choked; flow accelerates through the converging section, reaches its maximum speed at the throat, accelerates through the diverging section
and decelerates through the diverging section [12],[13].

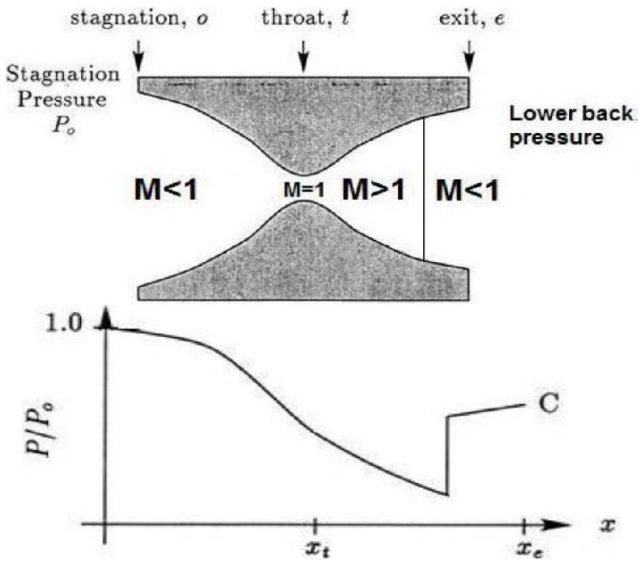

Fig. 2. Schematic view and a qualitative diagram of pressure versus the length axis for a converging-diverging nozzle with supersonic flow with shock wave.

As the matter of fact, a shock occurs after throat and the most important questions in this regard are where the shock actually happens and what the minimum pressure is after throat. To this end, there are several governing equations associated with converging-diverging nozzles that are taken into consideration in theoretical calculations, which also form the fundamentals of majority of computational fluid dynamics software such as ANSYS FLUENT®, which has been applied in this work [13].

Conservation of mass [12], [14]:

$\rho VA = \text{Constant}$ … (1)

Where ρ = density (kg/m3),
V= velocity (m/s), A = area (m^2).

Conservation of momentum [12], [14]:

$P_1A_1 + \rho_1 {V^2}_1 A_1 + \int_{A_1}^{A_2} Pda = P_2A_2 + \rho_2 {V^2}_2 A_2 \ldots$. (2)

Where V = velocity magnitude (m/s), p = pressure (N/m2 (Pa)

Conservation of energy[12], [15]:

$h_1 + \frac{{v^2}_1}{2} = h_2 + \frac{{v^2}_2}{2}$ ….(3)

In fact, the reason to use converging-diverging nozzles is to reach supersonic velocities to make the thrust even larger [16]. In converging nozzles sonic velocity is the highest velocity accessible with the extreme where h = enthalpy (kj/kg) point at the throat, while in converging-diverging nozzles due to the increase in volume after the throat in diverging area, density drops down which causes the velocity to augment even more and reach supersonic speeds [17], [18]. Manipulating the determinative variables such as area ratio and back pressure, the obtained Mach number at the end of the nozzle may be regulated. Important applications of the converging-diverging nozzle are aerodynamics especially in jet engines where high speed aircrafts or rocket engines work [19]. They play a significant role in a supersonic wind tunnel, where they draw air from a gas reservoir which might be either at atmospheric conditions or even contains compressed and pressurized air.

In this work a comprehensive simulation of a flow in a typical supersonic converging-diverging nozzle has been reported. Simulations have been carried out by ANSYS FLUENT® where meshing of geometries have been generated using ANSYS WORKBENCH. Two different turbulence models of k-ε and k-ω have been applied to the solution. Further on, the comparison of turbulence models, grid differentiation and computational methods have been analyzed and even compared to the experimental data to give better overview of the similar applications for future purposes. The outcomes of this research demonstrate an accurate enough coordination between the experimental data and the simulation results, which is exerted more to the 3D endeavors than 2Ds.

2. GEOMETRY AND THEORY

Converging-diverging nozzle has a non-swirling axisymmetric geometry. The 2D layout of the nozzle studied is illustrated in Fig. 3. High-pressure low velocity gas, which is air, flows through the convergent section in a subsonic condition and contracts in the throat. Then, the low- pressure high velocity air expands in divergent section in supersonic conditions [20]. Discretized method should be employed; therefore, the geometry in the shape of mesh has been developed in ANSYS WORKBENCH®.

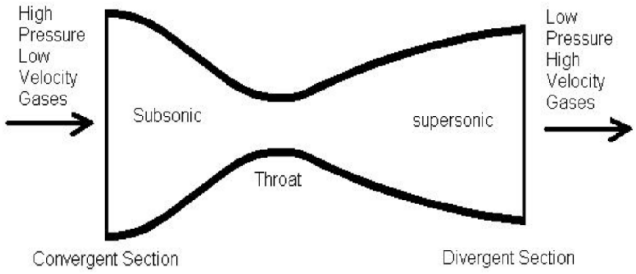

Fig. 3. 2D layout of the studied converging-diverging nozzle.

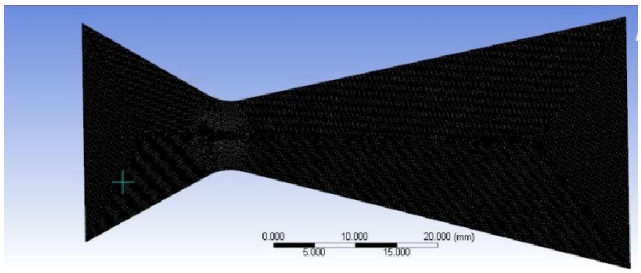

Fig. 4. Utilized geometries and meshes: a) 2D structured grid

In addition to the 2D structured grid, 2D complete (planner) case and 3D meshes were also generated to collate them in order to study the different cases. In terms of the type of mesh, the structured meshes were utilized for execution of the simulation. The simulations are resolved with a very fine mesh 0.0001 sizing for all the cases (mesh nodes 125153 and element 124157 in 2D cases) to predict the most accurate data. The schematic view of the studied grids is shown above fig 4,.

3. METHODOLOGY

Solver type was chosen as pressure-Based because fluid is compressible also high-speed flow. Different pressure inlets were examined i.e. 20, 19, 17, 16, and 14atm. The corresponding pressure outlets are then commonly for inlet condition 1atm. Note that, total pressure should be considered since total pressure is summation of static pressure and dynamic pressure and may be calculated as (4).

Evaluating the pressure value using by this formula,

$$\frac{P}{P_o} = \left(1 + \frac{\gamma-1}{2} M^2\right) \ldots (4)$$

The studied fluid is air, which must be defined as ideal gas; due to the supersonic flow density, that is not constant during passing through the nozzle.

Pressure-based solver is for low-speed incompressible flows, while density-based is mainly used for high-speed compressible flows. Both are now applicable to a broad range of flows (from incompressible to highly compressible), but the origins of the density-based formulation may give it an accuracy (i.e. shock resolution) advantage over the pressure-based solver for high-speed compressible flows [21]-[23] There are two most typical turbulence models used in CFD simulations, *k-ε* model & k-ω model. Both models are currently used for CFD. Sometimes, these two models have sizeable numerical differences. In most cases the difference is in convergence time and the number of iterations [24]. *k–ε* model is more feasible for fully turbulent flows. The model performs poorly for complex flows involving high pressure gradient, separation, and strong streamline curvature. The most significant weakness is lack of sensitivity to adverse pressure gradients. Basically, this model is suitable for initial iterations, initial screening of alternative designs, and parametric studies [25]. *K-ω* model allows for a more accurate near wall treatment with an automatic switch from a wall function to a low-Reynolds number formulation based on grid spacing. This model performs significantly better for complex boundary layer flows under adverse pressure gradient conditions. *K-ω* has significant advantages in numerical stability. This model underestimates the amount of separation for severe adverse pressure gradient flows [26].

However, based on the experience on the current case in Fluent, results for temperature are less sensitive to model choice and for velocity seem indifferent. Pressure results seem highly sensitive to both the model choice and the mesh. Two models are very different and it should be no surprise that some differences in consequences can be obtained from each model (this should be considered the norm rather than unusual).

4. RESULTS AND DISCUSSION

The pressure ratio over the nozzle and the temperature are 300K at exit and inlet 1300 K, respectively. For example take initial case from higher is, air flows from left hand side in 20 atm (2026500 Pa) then exits from right hand side after the nozzle in 1 atm (101325 Pa). The pressure ratio variation over the nozzle centerline gathered from the measurement is presented in TABLE, where and are instantaneous distance from the inlet and coordination of throat, respectively. While, p_0 (Pa) in inlet pressure. The cases are not performing under low Reynolds number; hence, *k–ε* model has been mostly used as the viscous model for all the present CFD calculations. However, other viscous models like *k-ω* were also examined and it was practically discovered that obtained results for temperature are less sensitive to model choice. However, the results for pressure were very sensitive to model choice.

TABLE I: GIVEN INLET AND OUTLET CONDITION DATA.

S.NO	Pressure inlet p_0 (Pa)	Wall	Pressure Outlet p (Pa)

1	14	No slip	1.01325
2	16	No slip	1.01325
3	17	No slip	1.01325
4	19	No slip	1.01325
5	20	No slip	1.01325

By the analysis of above table data is measure simulation in computational method and the results of given pressure value

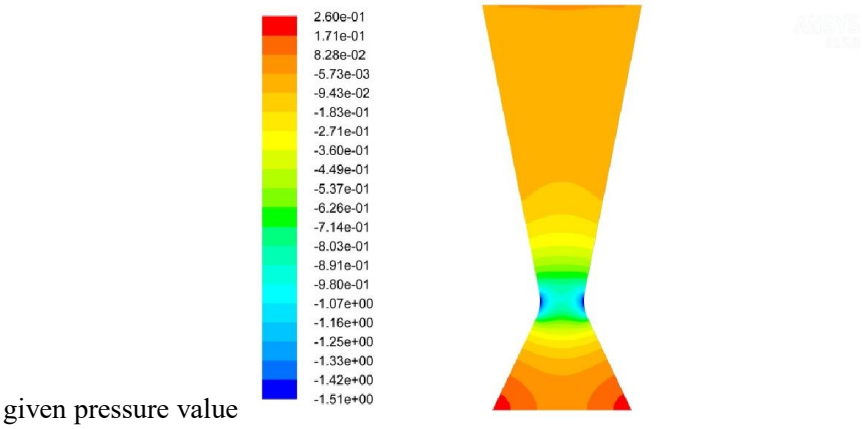

Fig 6, Contour of coefficient of pressure

Fig 6, in exhibiting the distinction the model values attain between the inlet and exit of the nozzle the given pressure value has getting changes high pressure in at inlet -1.51148,and then 0.25977 attain at outlet, for pressure value 14atm, and fig 7, the comparison of C_P between distance.

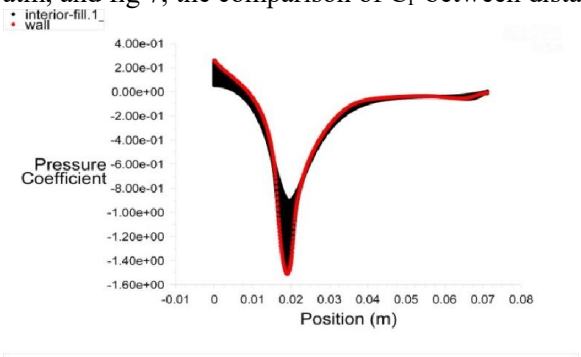

Fig 7, Plot for coefficient pressure (C_P).

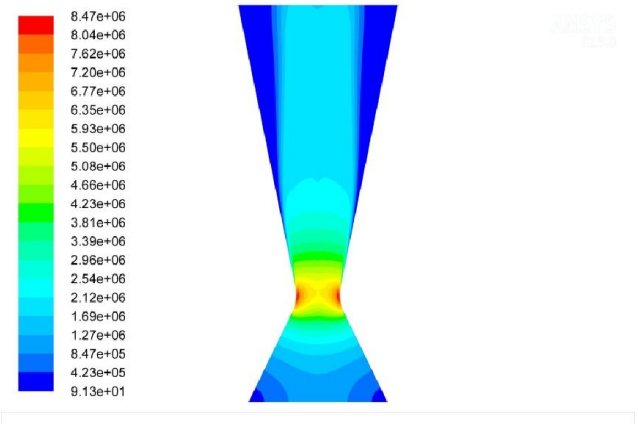

Fig 8, Contour of dynamic pressure (q),

If the contour values are to be giving pressure inlet 14atm, is calculated max 8466269, at throat difference up to 6343247.5.attain at throat area of the nozzle. fig 9, the total pressure contour has calculated for 14atm,attain maximum of exit upto 8345421pa. below the contour of total pressure.

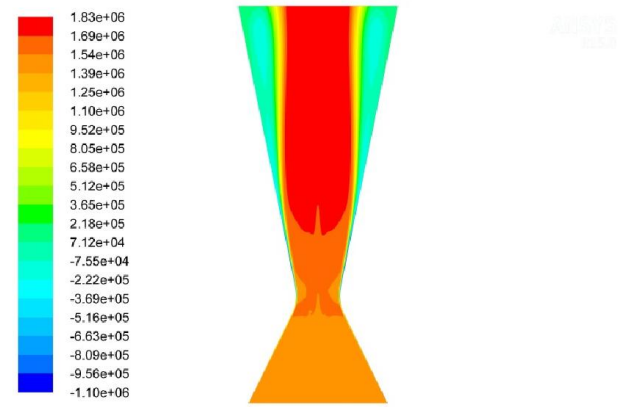

Fig 9, Contour of total pressure.(P_O)

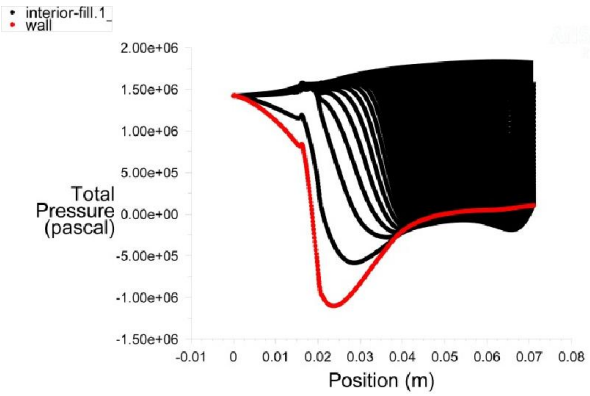

Fig 10, Plot for total pressure.

Above the fig 10, the total pressure plot 14atm min pressure value attains in at wall, as well as comparatively interior extends upto high above 18atm.

2. TABLE FOR MEASUREMENT OF TEMPERATURE

Sl no.	TEMP INLET (T_i)	TEMP OUTLET (T_e)
1.	1300k	2762k
2.	1350k	3310k
3.	1400k	3491k
4.	1450k	3613k
5.	1500k	3715k

Above table is measured for various temperatures for inlet conditions, but taking one sample for first inlet boundary condition. That condition fig 11, total pressure contour is below.

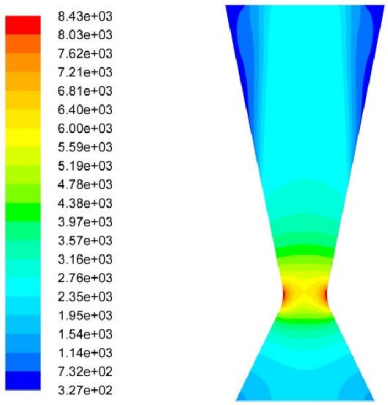

Fig 11, Contour of total temperature.(To)

At the throat the temperature achieved maximum of nozzle temperature up to 8432 k, in the exit of the nozzle center median temperature contour value 2762k, and then another graphical plot of total temperature contour is below.

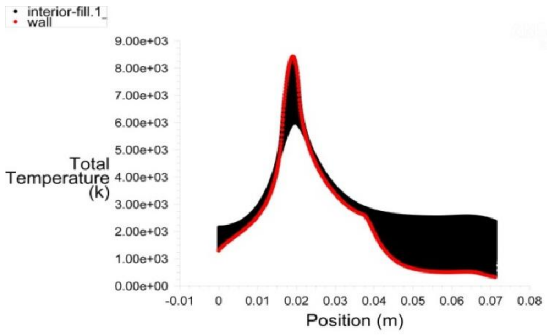

Fig 12, Plot for total temperature.

Fig 12, the temperature plot comparison which is given variation of temperature maximum to minimum between nozzle throat inlet and exit of the nozzle section by the value plotted distance in m, between total temperatures (k). Fig 13, the velocity minimum initialize min 1446.7m/s, after the flow run it attains at maximum of throat and exit value of 3714.3 m/s attain.

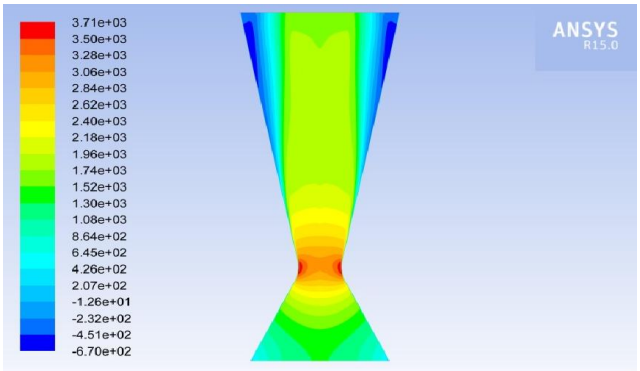

Fig 13, Contour of Y velocity.

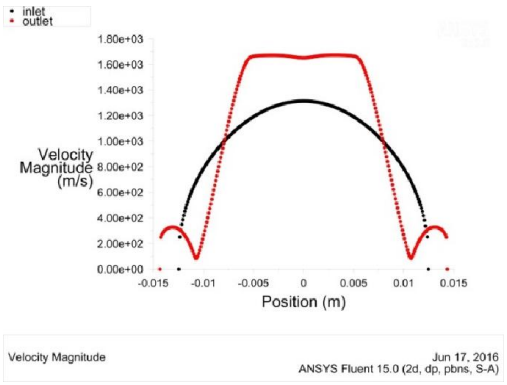

Fig 14, Plot for Y velocity.

Fig.14, the Y velocity magnitude is measure between distance m, the inlet condition getting peak from low to mid peak level of the plot is nearly 1446.7 m/s simultaneously the out value same case peak attain maximum of 3714.7 m/s at exit.

Fig 14 contours for Mach number and pressure were drawn. Unsurprisingly, Mach number at the throat increases slightly further until shock occurs but here the shock is not be occur, at where Mach number reaches on exit from inlet the flow didt get any changes. On the other hand, based on the contour of pressure, it is discovered that the trend of pressure change is closely similar. Moreover, analysis of the contour of wall shear stress demonstrates that the maximum shear stress happens at the throat, which is completely reasonable, and it decreases gradually through the diverging part of the nozzle toward the outlet. Before outlet the back pressure (flow reverse) occur at two edges of the nozzle exit.

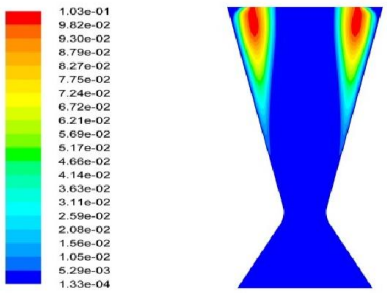

Fig 14, Contour for turbulence

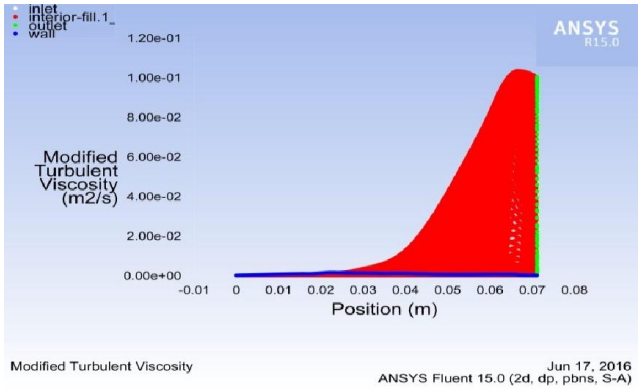

Fig 15, plot for turbulence.

Fig 15, above the turbulence plot is calculated for inlet to outlet of the nozzle and mainly the wall and interior case is priority calculation for turbulence

5. CONCLUSION

This thesis discuss about improving performance of an existing cd nozzle A-100. A-100 postures a simple design but also comprise an inferior efficiency than existing complex high classy nozzles. So by improving the efficiency of the A-100 nozzle it can be utilized for higher power required assignments. A-100 nozzle is designed in CATIA V5r20 and analysed in Ansys fluent. The velocity contour shows a highly accelerated profile up to 55%-60% of the nozzle divergent section. After 60% of nozzle length the air flow continues to decelerate proximate to the wall at a great extent. To make a reduction of this undesired phenomenon at the nozzle wall the length of the wall may be reduced to 50%, but there is a main problem if the reduction in nozzle length is made up to 50% it will make also an reduction in nozzle efficiency. This will also create a huge exhaust noise at the end. The turbulence contour specifies an introduction of heavy turbulence at 70% of the nozzle length nearer to divergent wall. Eliminating or making a reduction in this type of turbulent flow can improve the nozzle efficiency. To improve the nozzle efficiency it's almost impossible to reduce more than 40% of its length. This will also make a sharp fall in efficiency of the nozzle along with a huge noise creation at exhaust. Both are unacceptable hence to create an optimal design its length can be bring back to 80% of its original length along with 0.5° reduction in divergent angle. Introducing such a design modification can improve the efficiency of A-100 nozzle to a great extent. Thus an efficient nozzle can be utilized with less complicated design features. Implement of this design specification in real-time environment can be more cost effective. Hence this modified A-100 nozzle design is recommended for missiles and short range rockets.

REFRENCES

[1] T. Benson. (2013, July 25). Nozzle design, converging-diverging (CD) nozzle. National Aeronautics and space administration. [Online]. Available:https://www.grc.nasa.gov/www/k-12/airplane/nozzled.html.

[2] R. Boyanapalli *et al*., "Analysis of composite De-Laval nozzle suitable for rocket applications "*International Journal of Innovative Technology and Exploring Engineering*, vol. 2, pp. 336-344, 2013.

[3] T. W. Simpson *et al*., "Comparison of response surface and kriging models for multidisciplinary design optimization," *American Institute of Aeronautics and Astronautics*, vol. 98, pp. 1-16, 1998.

[4] J. J. Korte *et al.*, "Multidisciplinary approach to linear aerospike nozzle design," *Journal of Propulsion and Power*, vol. 17, pp. 93-98.

[5] D. Foque *et al.*, "Effects of nozzle type and spray angle on spray deposition in ivy pot plants," *Pest Manag Sci*, vol. 67, pp. 199-208.

[6] W. David and O. John, "SCORES - Web-based rocket propulsion analysis for space transportation system design," in *Proc. 35th Joint Propulsion Conference and Exhibit*, 1999.

[7] N. Zeoli *et al*., "CFD modeling of primary breakup during metal powder atomization," *Chemical Engineering Science*, vol. 66, pp. 6498-6504, 2011.

[8] T. Stevens *et al.*, *Steam Turbine Engineering*, MacMillan, 1906.

[9] W. J. Devenport. (March 1st, 2001). Nozzle applet. Applet. [Online]. Available:http://www.engapplets.vt.edu/fluids/CDnozzle/cdinfo.html.

[10] M. Darbandi and E. Roohi, "Study of subsonic–supersonic gas flow through micro/nanoscale nozzles using unstructured DSMC solver," *Microfluidics and Nanofluidics*, vol. 10, pp. 321-335, 2011.

[11] M. Einian. (2008). Compressible flow. CFD lab. University of Saskatchewan. [Online]. Available: http://www.engr.usask.ca/classes/ME/418/notes/T2-2008.ppt3] W. Devenport, R. Kapania, K. Rojiani, and K. Singh. (2012). Java applets for engineering education. Virginia Polytechnic Institute and State University. National Science Foundation. [Online]. Available: http://www.engapplets.vt.edu/fluids/CDnozzle/cdinfo.html.

[12] S. Fielding, "The basic equations of fluid dynamics," in *Laminar Boundary Layer Theory*, Durham University, 2013, pp. 1-7.

[13] S. Fielding, "Further equations of fluid dynamics," in *Laminar Boundary Layer Theory*, Durham University, 2013, pp. 37-44.

[14] R. L. Bayt *et al*., "Viscous effects in supersonic mems-fabricated micronozzles," in *Proc. the 3rd ASME Microfluids Symposium*, 1998.

[15] G. S. E. Antipas *et al*., "Microstructural characterisation of Al-Hf and Al-Li-Hf spray deposits," *Materials Characterization*, vol. 62, pp. 402-408, 2011.